

Predicting Future Lane Changes of Other Highway Vehicles using RNN-based Deep Models

Sajan Patel¹, Brent Griffin², Kristofer Kusano³, and Jason J. Corso^{1,2}

Abstract—In the event of sensor failure, it is necessary for autonomous vehicles to safely execute emergency maneuvers while avoiding other vehicles on the road. In order to accomplish this, the sensor-failed vehicle must predict the future semantic behaviors of other drivers, such as lane changes, as well as their future trajectories given a small window of past sensor observations. We address the first issue of semantic behavior prediction in this paper, by introducing a prediction framework that leverages the power of recurrent neural networks (RNNs) and graphical models. Our prediction goal is to predict the future categorical driving intent, for lane changes, of neighboring vehicles up to three seconds into the future given as little as a one-second window of past LIDAR, GPS, inertial, and map data.

We collect real-world data containing over 500,000 samples of highway driving using an autonomous Toyota vehicle. We propose a pair of models that leverage RNNs: first, a monolithic RNN model that tries to directly map inputs to future behavior through a long-short-term-memory network. Second, we propose a composite RNN model by adopting the methodology of Structural Recurrent Neural Networks (RNNs) to learn factor functions and take advantage of both the high-level structure of graphical models and the sequence modeling power of RNNs, which we expect to afford more transparent modeling and activity than the monolithic RNN. To demonstrate our approach, we validate our models using authentic interstate highway driving to predict the future lane change maneuvers of other vehicles neighboring our autonomous vehicle. We find that both RNN models outperform baselines, and they outperform each other in certain conditions.

I. INTRODUCTION

Autonomous vehicles are equipped with many advanced sensors that allow them to perceive other vehicles, obstacles, and pedestrians in the environment. Substantial work using autonomous vehicles and other forms of robots in the areas of perception and reasoning to allow these agents to make decisions based on their percepts exists. However, the majority of this work makes an obvious assumption: the sensors are working reliably. Under sensor failure, the ability to make autonomous decisions is lost. In practice, such an assumption is risky and not always a guarantee, especially in the case of autonomous vehicles deployed in the real world amongst other human-driven vehicles. In the event of sensor failure in autonomous vehicles, only past sensor readings are available for decision making. These vehicles then need to be able to

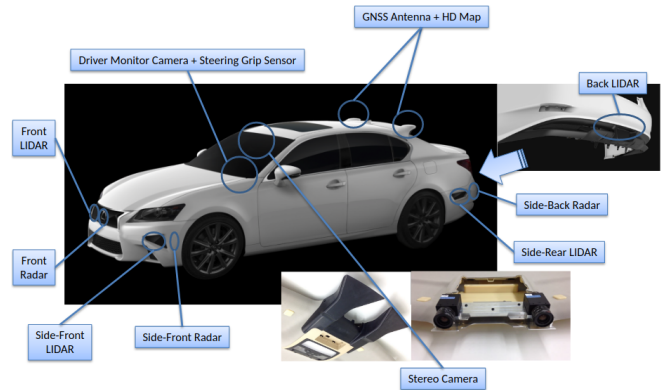


Fig. 1. The Toyota autonomous vehicle used for data set collection and experimentation. The sensor suite contains a multi-LIDAR system along with GPS and inertial sensors. A stereo camera is also included and used for visualizations, but it is not used in the data set for this work.

plan and execute emergency maneuvers while safely avoiding other moving obstacles on the road.

To optimally execute emergency maneuvers requires the knowledge of what other vehicles surrounding the *blinded agent* are going to do in the near future. One form this task takes is the prediction or anticipation of future semantic maneuvers and corresponding paths of each neighboring vehicle. In this work, we specifically address the first issue of predicting the maneuvers of other vehicles up to three seconds into the future, such as performing left or right lane change maneuvers or staying in the same lane, while driving on the highway. We do so using as little as one-second and up to five-seconds of past observations of neighboring vehicles based on LIDAR, GPS, inertial, and high-definition map data collected from an autonomous Toyota vehicle (see Fig. 1). As opposed to vision systems, LIDAR is a widely used and proven system for sensing that provides reliable measurements for tracking vehicles, pedestrians, and other objects surrounding autonomous car [1]. In this paper, the LIDAR-based sensing is considered a black box.

The choice of modeling paradigm is an interesting one for this problem. We need a paradigm that can capture the way various measurements relate to each other and evolve over time, and, at the same time, we need one that can learn from the heaps of data that is available. The classical approach to handle the former need is probabilistic graphical models [2] such as factor graphs, spatiotemporal graphs and dynamic Bayesian networks [3], which bring graphical models into the sequential modeling space. Probabilistic graphical models are widely used in the robotics community for many reasons,

¹ Robotics Institute, University of Michigan, Ann Arbor
{sajanpt1, jjcorso}@umich.edu

² Electrical Engineering and Computer Science, University of Michigan, Ann Arbor {griffb, jjcorso}@umich.edu

³ Toyota Motor North America Research and Development, Ann Arbor
kris.kusano@toyota.com

including their interpretability and the high level structures, which can capture various relationships between features to modeling temporal sequences. However, they require a parameterization of factor models that is structured by hand using domain-specific knowledge and optimized using various methods, including structural support vector machines and expectation maximization [4], which, arguably, struggle to incorporate large-scale data well.

On the other hand, recent advancements in temporal sequence modeling have come from the use of recurrent neural networks (RNNs) [5], [6], which can be trained end-to-end for various tasks. While methods that rely on deep learning lack the interpretability of factor graphs, these networks learn richer models than those currently employed in factor graphs. Indeed, RNN-based methods have been applied to predicting future vehicle maneuvers but only in the context of making predictions for a single observed human driver [7], [8].

In this work, we want both the interpretability of factor graphs and the scalability of deep RNNs. To that end, we bring RNN-based methods to the problem of predicting the future maneuvers of *all other* vehicles within the vicinity of our own autonomous vehicle while traveling on a highway.

First, we propose a standard RNN-based architecture for predicting the future lane change maneuvers of other highway vehicles. This architecture implements a long-short-term-memory (LSTM) model, which we call a *monolithic RNN* for reasons that will soon be clear. It handles the scalability issue and can learn from our large set of data in an end-to-end fashion. However, it does not afford any level of interpretability that graphical models do.

To overcome this limitation, we propose a second RNN-based model, which we call a *composite RNN* that leverages the recent work in structural RNNs [8]. Here, RNN units are connected in the form of factor graphs. These networks employ the interpretable, high-level spatiotemporal structure of graphical models while using RNN units specifically to learn rich, nonlinear factor and node functions for factor graphs. As with single RNN-based networks, Structural RNNs are trained end-to-end and can be unrolled over each step in the temporal sequence at inference time to make the predictions for the given task. Following the methodology of Structural RNNs, we convert our proposed lane-based graphical model into a Structural RNN so we can learn rich factor models for lane change prediction.

Our composite RNN captures the spatiotemporal interactions between a given vehicle and its neighbors in the same and adjacent lanes. To model lane-wise interactions, the graph includes a factor for the right, left, and same lanes that combines pose and map-based lane information for the neighboring vehicles within the given lane. The model is unrolled over each time step of the sequence of past sensor observations to predict the future lane change maneuver class.

The main contributions of our work are the RNN-based model:

- 1) We propose an RNN-based model for the lane change prediction task, using long-short-term-memory-based

RNNs. We call this the monolithic RNN.

- 2) We develop a graphical model that captures the temporal evolution of neighboring highway vehicles and their lane-based spatial interactions to predict future lane change maneuvers. We transform our graphical model into a Structural RNN to learn factor functions from data. We call this the composite RNN.

We provide an analysis on the efficacy of prior and post current-time window size for both our single RNN-based network and Structural RNN in predicting the future behavior of all tracked highway vehicles in alternative lanes, not just forward and backward in the same lane, in the event of sensor malfunction. We train and evaluate our models using over 500,000 instances of natural multi-lane interstate highway driving data obtained from an autonomous vehicle driving amongst other human drivers. This data set is not augmented with simulated driving scenarios as in [9] and is more extensive than other highway datasets used in [8], [7]. Thus, the performance of our models on this data set constitutes the performance of our models on the actual autonomous robot for authentic highway driving.

Additionally, to the best of our knowledge, this is the first paper to use deep learning ideas to predict lane change maneuvers of other vehicles.

II. RELATED WORKS

A. Maneuver Anticipation

Recent work in predicting driver maneuvers has primarily focused on the intent of the target vehicle's human driver; intent is based on tracking the driver's face with an inward-facing camera along with features outside of and in front of the vehicle using a camera, velocity sensor, and GPS [8], [7], [4]. The works presented in [8], [7] use various RNN-based architectures and [4] uses graphical models, which are essential to this work; however, rather than anticipating the behavior of our own vehicle, we address the problem of predicting the lane change maneuvers of neighboring vehicles in an interstate highway environment. Moreover, by utilizing a multi-LIDAR system that provides all-around coverage, we predict future maneuvers for multiple vehicles in the surrounding neighborhood rather than only those detected and tracked in front of the data collection vehicle. Additionally, our data set does not contain any vision input and our methods work at the level of vehicle detections rather than raw sensor input.

The method in [9] involves anticipating the maneuvers of other vehicles and takes a reinforcement learning approach to simulate multiple possible future maneuvers and chooses the ones that are most likely to occur; however, this approach is based on simulated approximations of limited highway driving scenarios. Conversely, our method is trained and evaluated on data collected from natural freeway driving, which keeps our validation unaffected by simulation-based modeling errors.

B. Graphical Models and Structural RNNs

Graphical models are used in [4] in the form of autoregressive input-output Hidden Markov Models (HMMs) to model the temporal sequences that lead up to various maneuvers. Similarly, HMMs are used in [10] using a similar neighborhood context for the target vehicle; however, [10] relies on hand-tuned features computed from the tracked poses and map information of all of the vehicles rather than learning the factor models without restrictive assumptions on what features to extract. The work presented in [8] bridges the gap between probabilistic graphical models and deep learning by introducing the Structural RNN, which exhibits better performance over graphical model counterparts through evaluations in many problem spaces, including maneuver anticipation for the target vehicle’s human driver using facial tracking. While our method follows the same methodology of transforming a graph into a Structural RNN, we propose a novel graph that takes into account lane-based spatiotemporal interactions between vehicles in the neighborhood of the target vehicle to predict future lane change maneuvers. We also evaluate the performance solely on natural freeway driving rather than city driving.

III. PROBLEM SET-UP AND DATA

Our goal is to predict the lane-changing behavior of vehicles other than the ego-vehicle given a recent history of sensor readings varying from one to five seconds and a goal prediction horizon varying from one to three seconds. Our prediction space is either left-lane change, right-lane change, or no-lane change. We collect a data set of over 500,000 samples of highway driving using a Toyota sedan retrofitted with sensors of a typical automated vehicle. In this paper, we will refer to this vehicle as the ego vehicle, shown in Figure 1. The sensor suite includes 6 ibeo LUX 4L LIDARs mounted on all sides of the ego vehicle as well as an Applanix POS LV (version 5) high-accuracy GPS with Real-Time Kinetic (RTK) corrections. Using the ibeo LUX Fusion System [11], we detect the relative position and orientation of neighboring vehicles up to approximately 120 meters away.

Using high-definition maps that include lane-level information (e.g. lane widths, markings, curvature, GPS coordinates, etc.) along with GPS measurements and the relative detections of neighboring vehicles, we localize the ego vehicle and its neighbors on the map. The GPS coordinates of the ego vehicle are projected into a world-fixed frame using the Mercator projection [12], and the relative poses of other vehicles are also mapped into this frame to determine absolute poses. Along with vehicle poses, the maps allow us to determine the lane in which the ego and neighboring vehicles are traveling in. All of this data are collected at 25 Hz in Southeast Michigan multi-lane highways.

Given these off-the-shelf methods for detecting other vehicles and localizing them to the map, we focus on developing a framework that uses pose and lane information. Specifically, we represent the i^{th} vehicle at each time step t

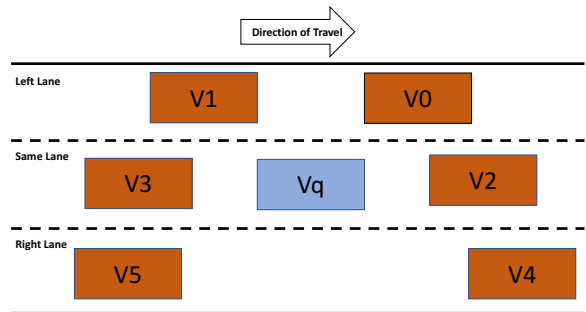


Fig. 2. An example six-car (three-lane) context of neighbors surrounding the target vehicle. We chose a six-car neighborhood since it is the minimal context required for representing the lane-based interactions between the observed vehicles. All of these neighboring vehicles are not present at each time step in natural freeway driving; thus, indicator variables are included as a part of the augmented vehicle states used as inputs to our model.

with the following state vector:

$$v_t^i = [P_{x_t}^i, P_{y_t}^i, \psi_t^i, n_l, n_r, n_t]^T, \quad (1)$$

where P_x and P_y are the absolute world-fixed frame positions in meters, ψ is the heading angle of the vehicle in radians, n_l is the number of lanes to the left of the vehicle, n_r is the number of lanes to the right of the vehicle, and n_t is the number of total lanes on the highway in the vehicle’s direction of travel. We represent the sequence of historical states over time for each vehicle as

$$V_t^i = [v_{t_h}^i, \dots, v_t^i], \quad (2)$$

where t_h is the maximum number of historical time steps included. For each vehicle at each time step, there are three possible lane change maneuvers that can occur t_f time steps into the future—left lane change, right lane change, and no lane change. We denote this set of possible maneuvers as $\mathcal{M} = \{left, right, same\}$. These are determined by examining the change in lane identifiers provided in the map between times t and t_f . We represent these labels as one-hot vector $y_{t_f}^i$ in (1) for each sample and annotate each vehicle sample V_t^i in (2) with its future lane change label vector.

IV. LANE CHANGE PREDICTION MODELS

For a given vehicle v_q traveling on a multi-lane highway, we model the future lane change possibility as a function of the vehicle’s previous states as well as the previous states of its neighboring vehicles. We use a six-vehicle neighborhood, shown in Fig. 2, that contains the vehicles ahead and behind the target vehicle in the left and right lanes and the vehicles directly ahead and behind the target vehicle in the same lane. According to this convention, for every target vehicle v^q , the neighbors ahead and behind it in the left lane are v^0 and v^1 , the neighbors ahead and behind it in the same lane are v^2 and v^3 , and the neighbors ahead and behind it in the right lane are v^4 and v^5 .

Since v^q may be at the right- or left-most lane or other vehicles may be out of sensor range during natural freeway driving, it is not guaranteed that each of these neighboring

positions is actually occupied by a vehicle. For this reason, we only include a neighborhood of six vehicles, which provides a minimalist representation of the target vehicle's context. Accordingly, we augment the state of each neighboring vehicle v^j from each time step t_h to t with an indicator variable of 1 for when it is present in the target vehicle's neighborhood and 0 for when it is not.

A. Monolithic RNN for Lane-based Maneuver Prediction

The simpler of the two RNN-based models that we propose uses a single long-short-term-memory-based RNN or LSTM [6] which we call the monolithic RNN. As input at each time step, the LSTM takes in the concatenation of all of the vehicle states. The output at each time step is a recurrent context vector c_t and embedding h_t . As shown below, the LSTM is unrolled across all time steps $k \in [t_h, t]$.

$$(h_k, c_k) = LSTM([v_k^0; \dots; v_k^5; v_k^q], h_{k-1}, c_{k-1}) \quad (3)$$

where h_0 and c_0 are zero initialized before each forward pass through the network. After unrolling all time steps of vehicle states through the LSTM, we take the output of the last time step h_t and pass it through two fully connected layers and a softmax layer to obtain the final lane change prediction for the target vehicle as follows:

$$f_t = \sigma(W_1 h_t^n + b_1), \quad (4)$$

$$y_{t_f}^q = \text{softmax}(W_2 f_t + b_2), \quad (5)$$

where W and b are the weights and biases of the fully connected layers, σ is the sigmoid function used as the nonlinear activation function for the first fully connected layer, and the softmax function is given in [13], [14]. The model is trained end-to-end, and we use the softmax cross-entropy loss as our classification loss function [13], [14]. However, as we noted earlier, although this LSTM-based model is sequential and can leverage the end-to-end training nature of deep networks, it is opaque and hard to understand what is actually happening inside of it. In the next section, we discuss the more sophisticated RNN-based model we propose, which allows us to transparently model that problem using factor graphs and, at the same time, compose the factors together into an RNN-based model.

B. Graphical Models for Lane-Based Maneuver Prediction

Given the three-lane structure of the target vehicle's neighborhood, we design a factor graph that represents the probability of the future lane change label using edges that represent the interaction between vehicles in each lane (left, same, right) with the target vehicle. We make the assumption that given the current observed state of the target vehicle, the vehicles in a given lane are conditionally independent of vehicles in other lanes. Hence, we model factors for vehicles in the left, right, and same lanes separately. Furthermore, we assume that the maneuver is conditioned on the physical states of the vehicles within the three-lane context. The random variables are the maneuver labels Y and the future vehicle states; however, only the future maneuver label is of interest. We start with the joint distribution over the target

vehicle's maneuver labels and the states of all vehicles within the context from times t_h to t and use our assumptions to model the probability of the label Y_{t_f} taking on value $m \in \mathcal{M}$ as follows:

$$\begin{aligned} P(Y_{t_f} = m, y_t, \dots, y_{t-t_h}, V_t^q, V_t^0, \dots, V_t^5) & \quad (6) \\ &= \sum_{y_{t_f} \in \mathcal{M}/m} P(y_{t_f}, y_t, \dots, y_{t-t_h}, V_t^q, V_t^0, \dots, V_t^5) \\ &= \sum_{y_{t_f} \in \mathcal{M}/m} P(v_{t_h}^q, v_{t_h}^0, \dots, v_{t_h}^5) \times \\ & \quad \prod_{k=t_h}^t \left(P(y_{k+1} | v_k^q, v_k^0, \dots, v_k^5) \right. \\ & \quad \left. \times P(v_k^q, v_k^0, \dots, v_k^5 | v_{k-1}^q, v_{k-1}^0, \dots, v_{k-1}^5) \right) \end{aligned}$$

We further factorize the distributions in (6) based on our assumption of conditional independence between lanes and Markovian temporal dynamics:

$$\begin{aligned} P(y_{k+1} | v_k^q, v_k^0, \dots, v_k^5) & \quad (7) \\ &= P(y_{k+1} | v_k^q, v_k^0, v_k^1) P(y_{k+1} | v_k^q, v_k^2, v_k^3) \times \\ & \quad P(y_{k+1} | v_k^q, v_k^0, v_k^4, v_k^5) \\ &= \phi_l(y_{k+1}, v_k^q, v_k^0, v_k^1) \phi_s(y_{k+1}, v_k^q, v_k^2, v_k^3) \times \\ & \quad \phi_r(y_{k+1}, v_k^q, v_k^4, v_k^5) \end{aligned}$$

$$\begin{aligned} P(v_k^q, v_k^0, \dots, v_k^5 | v_{k-1}^q, v_{k-1}^0, \dots, v_{k-1}^5) & \quad (8) \\ &= P(v_k^q, v_k^0, v_k^1 | v_{k-1}^q, v_{k-1}^0, v_{k-1}^1) \\ & \quad \times P(v_k^q, v_k^2, v_k^3 | v_{k-1}^q, v_{k-1}^2, v_{k-1}^3) \\ & \quad \times P(v_k^q, v_k^4, v_k^5 | v_{k-1}^q, v_{k-1}^4, v_{k-1}^5) \\ &= \gamma_l(y_{k+1}, v_k^q, v_k^0, v_k^1) \gamma_s(y_{k+1}, v_k^q, v_k^2, v_k^3) \\ & \quad \times \gamma_r(y_{k+1}, v_k^q, v_k^4, v_k^5) \end{aligned}$$

where each function $\phi(\cdot)$ and $\gamma(\cdot)$ is a parameterization of the spatiotemporal and temporal factor functions, respectively, and where l , r , s denote the left, right, and same lanes. These functions can take on various forms, include exponential models in the case of the spatiotemporal factors and Gaussians in the case of the temporal models [2]. By parameterizing each of the three lane factors using the states of each of the neighboring cars in the lane along with the target vehicle, we allow the model to take into account spatiotemporal interactions between each of the vehicles used in each factor. The final lane change prediction is given by

$$y_{t_f}^q = \underset{m \in \mathcal{M}}{\operatorname{argmax}} P(Y_{t_f} = m, y_t, \dots, y_{t-t_h}, V_t^q, V_t^0, \dots, V_t^5). \quad (9)$$

C. Learning Factor Functions using Structural RNNs

Factor functions are typically parameterized by hand to incorporate hand-tuned features with simple weights, which limits the modeling power of standard factor graphs [8], [7], [15]. Following the approach of [8], we preserve the transparency of the graphical model and, yet, leverage the power of RNNs by converting it into a Structural RNN

(SRNN) and train it to classify the lane change label. The SRNN composites factors, captured as network snippets, into a larger RNN. This allows us to use the sequence modeling power of RNNs together with the structure provided by our spatiotemporal factor graph.

To convert our graph into a Structural RNN, we use LSTM units to represent each of the three lane interaction factors (each $\phi(\cdot)$ in (7)) as *factorRNNs*. While standard Structural RNNs use different LSTM units for each spatiotemporal and temporal factor as in [8], we note that a single LSTM unit can jointly model both the spatiotemporal factors along with temporal factors (each $\gamma(\cdot)$ in (8)). LSTM units have two recurrent functions within them—one for computing the output h_k and one for computing the context vector c_k at each time step given the input features (vehicle states) and previous outputs and states h_{k-1} and c_{k-1} [6]. This allows us to model the spatiotemporal interaction factors with the recurrent output function since the outputs of those are directly used in the prediction of the future lane change label. Similarly, we use the recurrent context vector function within each LSTM to model temporal factors as a function of the input vehicle states. By using a single LSTM to model both factors for each lane, we reduce the complexity of our model and benefit from being able to train it with a smaller dataset.

Since our graph has a single random variable node representing the future lane change maneuver, our Structural RNN has one *nodeRNN* to combine the outputs of each *factorRNN*. During the forward pass of the Structural RNN, each vehicle state at each time step are passed through the *factorRNNs*, whose outputs are concatenated and then passed through the *nodeRNN*. The following equations detail the computation performed at each time step, noting that h_t^i is the output of the i^{th} RNN unit at time step $k \in [t_h, t]$, and that the scripts l, r, s , and n mean left lane, right lane, same lane, and node, respectively:

$$(h_k^l, c_k^l) = LSTM_l([v_k^0; v_k^1; v_k^q], h_{k-1}^l, c_{k-1}^l), \quad (10)$$

$$(h_k^s, c_k^s) = LSTM_s([v_k^2; v_k^3; v_k^q], h_{k-1}^s, c_{k-1}^s), \quad (11)$$

$$(h_k^r, c_k^r) = LSTM_r([v_k^4; v_k^5; v_k^q], h_{k-1}^r, c_{k-1}^r), \quad (12)$$

$$(h_k^n, c_k^n) = LSTM_n([h_k^l; h_k^s; h_k^r], h_{k-1}^n, c_{k-1}^n). \quad (13)$$

As with the monolithic LSTM model, the output for the final time step t of the *nodeRNN* is then fed through two fully connected layers using equations (4) and (5) to get the final lane change prediction y_{t+f}^q , noting that the weights and biases are unique to each model. The complete architecture is shown in Fig. 3; the model is trained end-to-end, and we use the softmax cross-entropy loss as our classification loss function.

D. Implementation Details

Both our proposed monolithic LSTM and SRNN models are implemented using LSTMs with layer normalization [16]. All LSTM units within the SRNN and the monolithic LSTM have a hidden state size of 128. The first fully connected layer in each network has an input and output size of 128. The seconds fully connected layer in both has an input size of 128 and output size of $|\mathcal{M}| = 3$. During training, we

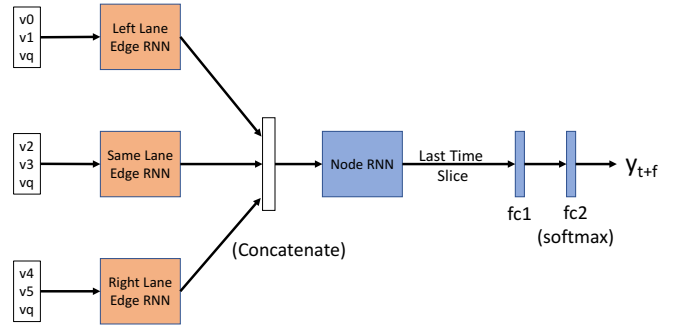


Fig. 3. Our composite RNN model created using our lane-based factor graph from Section IV-B. At each k , the states for each neighboring car for the given lane and the target car are concatenated and fed as input through the given lane’s edge RNN. Each edge RNN output is concatenated and fed through the node RNN. Once the network is unrolled across all the past t_h observations, the last node RNN output is fed through two fully connected layers to get the final lane change maneuver classification.

use 20% weight dropout in the LSTM units as implemented in [17]. We optimize the softmax cross-entropy loss using the ADAM optimizer [18] with a learning rate of 0.001. All of our software for our proposed models is implemented in Python using Tensorflow [19].

V. EXPERIMENTS

A. Setup

We use the data set collected by our autonomous vehicle (Sec. III) for evaluation. For a given time history and future prediction horizon, we sample all the target vehicles tracked long enough to satisfy these time requirements and split up the data set into a training and evaluation set. In natural freeway driving scenarios, no-lane change events outnumber the number of left-lane and right-lane change events; thus, we manually balance each training set to contain roughly equal numbers of left-lane, right-lane, and no-lane change samples. We use the authentic, unbalanced evaluation set to test our models.

B. Comparison with Classical Baselines

In our first experiment, we evaluate the performance of our monolithic LSTM and composite SRNN models against two classical baselines, logistic regression and linear support vector machines (SVM) [14], for time histories (t_h) of one and three seconds and future prediction windows (t_f) of one and three seconds. Both classical models are implemented in a one-vs-all multi-class classification setting and are trained on a subset of the balanced training data that filters away outliers. Both models use the hand-tuned features of the relative in-lane distance, relative velocity, and time-to-collision [20] between the target vehicle v^q and its neighboring vehicles at instantaneous time steps of zero and one second into the past when $t_h = 1s$ and zero, one, two, and three seconds into the past when $t_h = 3s$. During training, we post-process the prediction thresholds to maximize the f1-score of the models [14], [7]. Our proposed models are trained using the original balanced training data for each setting of t_h and t_f and have no post-processing of prediction thresholds. In this

TABLE I
EVALUATION FOR NEIGHBORING VEHICLE LANE CHANGE MANEUVER PREDICTION ON AUTHENTIC HIGHWAY DRIVING

Model	th	tf	Left		Right		Same		Overall Accuracy	Lane Only Accuracy	Balanced Accuracy
			Precision	Recall	Precision	Recall	Precision	Recall			
Logistic Regression	1	1	0.010	0.074	0.000	0.000	0.983	0.956	0.940	0.026	0.343
Linear SVM	1	1	0.010	0.074	0.000	0.000	0.983	0.955	0.940	0.026	0.343
LSTM (<i>ours</i>)	1	1	0.015	0.033	0.011	0.963	0.982	0.028	0.039	0.632	0.341
SRNN (<i>ours</i>)	1	1	0.014	0.028	0.011	0.959	0.981	0.981	0.031	0.629	0.656
Logistic Regression	1	3	0.004	0.001	0.000	0.000	0.956	0.997	0.953	0.0003	0.333
Linear SVM	1	3	0.005	0.001	0.031	0.044	0.957	0.956	0.916	0.030	0.334
LSTM (<i>ours</i>)	1	3	0.041	0.051	0.029	0.955	0.951	0.020	0.048	0.645	0.342
SRNN (<i>ours</i>)	1	3	0.047	0.034	0.029	0.958	0.955	0.028	0.054	0.641	0.340
Logistic Regression	3	3	0.015	0.074	0.000	0.000	0.957	0.930	0.892	0.025	0.335
Linear SVM	3	3	0.014	0.048	0.019	0.000	0.957	0.951	0.911	0.016	0.333
LSTM (<i>ours</i>)	3	3	0.021	0.041	0.029	0.904	0.961	0.076	0.099	0.621	0.340
SRNN (<i>ours</i>)	3	3	0.034	0.035	0.028	0.905	0.962	0.082	0.105	0.611	0.341

Note: th refers to time history; tf refers to future time prediction horizon.

TABLE II
EVALUATION FOR TIME-HORIZON FOR PROPOSED MODELS

Model	th	tf	Overall Accuracy	Lane-Only Accuracy	Balanced Accuracy
LSTM	1	1	0.039	0.632	0.341
SRNN	1	1	0.031	0.629	0.656
LSTM	1	2	0.028	0.633	0.337
SRNN	1	2	0.048	0.633	0.337
LSTM	1	3	0.048	0.645	0.342
SRNN	1	3	0.054	0.641	0.340
LSTM	3	1	0.094	0.590	0.334
SRNN	3	1	0.098	0.584	0.332
LSTM	3	2	0.092	0.609	0.342
SRNN	3	2	0.103	0.605	0.344
LSTM	3	3	0.099	0.621	0.340
SRNN	3	3	0.105	0.611	0.341
LSTM	5	1	0.121	0.598	0.357
SRNN	5	1	0.161	0.568	0.353
LSTM	5	2	0.173	0.559	0.343
SRNN	5	2	0.187	0.553	0.344
LSTM	5	3	0.129	0.573	0.336
SRNN	5	3	0.195	0.541	0.336

Note: th refers to time history; tf refers to future time prediction horizon.

experiment, all models are evaluated on the full, authentic evaluation data set. Table I presents the results; metrics in the table are explained in Sec. V-D and Analysis is in Sec. VI.

C. Impact of Time Horizons on Proposed Models

Using the proposed models only, we further analyze the impact of the history and future time horizons. We choose a variable time history of one, three, of five seconds and a future prediction window of one, two, or three seconds. We train both models from scratch for each combination of t_h and t_f on the balanced training set and evaluate on the unbalanced evaluation set. Table II presents these results.

D. Results

The precision, recall, and accuracies for predicting left, right, and no lane change (same lane) maneuvers for our

proposed models and classical baselines evaluated on authentic highway driving are shown in Table I. We compute the number of true positives tp_m , false positives fp_m , and false negatives fn_m for each maneuver $m \in \mathcal{M}$, and compute the precision Pr_m and recall Re_m values as $Pr_m = tp_m / (tp_m + fp_m)$ and $Re_m = tp_m / (tp_m + fn_m)$, respectively. We also calculate the overall accuracy of the models, although it is not very useful since the vast majority of the cases are no-lane change. To overcome this limitation, we calculate two other summary measures. The balanced accuracy is a class averaged accuracy over the three cases, equally weighting the left-lane, right-lane and no-lane change accuracies. And, we compute the accuracy for the subset with the no-lane change samples completely discarded (Lane Only Accuracy).

VI. ANALYSIS

From our experiment comparing our proposed monolithic LSTM and composite SRNN models with classical logistic regression and linear SVM baselines, we see that the RNN-based models outperform the classical models overall. Both of our proposed models exhibit higher lane only accuracy. Across all of our evaluated t_h and t_f settings, the classical baselines have a lower balanced accuracy. This highlights the limitations of logistic regression and linear SVMs in their ability to learn how to predict right and left lane changes; rather, they learn to predict no lane change, which is the prior for natural highway driving. Both the LSTM and SRNN models in this regard learn useful embeddings or composite factors that allow it to predict the more rare cases of left and right lane changes for other vehicles when applied to authentic driving scenarios.

Our analysis of the impact of different time horizons shows mixed cases for lane only and balanced accuracies. The SRNN models has comparable performance with the monolithic LSTM w.r.t. balanced accuracy, showing that the use of an interpretable structure imposed from a factor graph model is similar to the unstructured and uninterpretable monolithic LSTM, begging the unanswerable question if the LSTM is inducing the same terms specified in the factor graph. While the monolithic LSTM has higher lane only

accuracies across all time settings, the SRNN has very similar balanced accuracies for the longer time histories of three and five seconds. Interestingly, for the case of $t_h = 1s$ and $t_f = 1s$, our SRNN model outperforms our monolithic LSTM model in balanced accuracy.

VII. CONCLUSION AND FUTURE WORK

We have presented a suite of methods for modeling and inferring future lane change maneuvers expected to be made by neighboring vehicles in highway settings. We propose two recurrent neural network-based models in the analysis; one is a monolithic LSTM and the other is a composite RNN that uses Structural RNNs to map a transparent factor graph into a RNN architecture. Our results and subsequent analysis show detailed evidence that, first, these models exhibit good performance of lane change prediction of other vehicles and, second, these both have merit for different time horizon settings. Given the transparency of the composite model, we select this as the new model of choice over the more opaque monolithic LSTM. While this work specifically focuses on the problem of maneuver anticipation on interstate highways, in which the key semantic maneuvers are limited to lane change, we note that our methods can be extended to a more diverse set of maneuvers present in city driving as well, such as turning at intersections. Since much of the problem for maneuver anticipation for *other* vehicles besides the given target vehicle based only on past LIDAR and inertial data has been unexplored, we leave the extensions for city driving and more diverse maneuvers for our future work.

ACKNOWLEDGEMENT

This work was sponsored by Toyota Motor North America Research and Development (TMNA R&D). We would like to acknowledge TMNA R&D for providing the collected data set using the Toyota Highway Teammate vehicle. We also would like to acknowledge Richard Frazin for his help in processing the data set and in developing baseline linear models.

REFERENCES

- [1] J. Levinson, J. Askeland, J. Becker, J. Dolson, D. Held, S. Kammel, J. Z. Kolter, D. Langer, O. Pink, V. Pratt, *et al.*, "Towards fully autonomous driving: Systems and algorithms," in *Intelligent Vehicles Symposium (IV), 2011 IEEE*. IEEE, 2011, pp. 163–168.
- [2] D. Koller and N. Friedman, *Probabilistic graphical models: principles and techniques*. MIT press, 2009.
- [3] K. Murphy, "Dynamic Bayesian Networks: Representation, Inference and Learning," Ph.D. dissertation, University of California at Berkeley, Computer Science Division, 2002.
- [4] A. Jain, H. S. Koppula, B. Raghavan, S. Soh, and A. Saxena, "Car that knows before you do: Anticipating maneuvers via learning temporal driving models," in *The IEEE International Conference on Computer Vision (ICCV)*, December 2015.
- [5] K. Cho, B. van Merriënboer, C. Gulcehre, F. Bougares, H. Schwenk, and Y. Bengio, "Learning phrase representations using rnn encoder-decoder for statistical machine translation," in *Conference on Empirical Methods in Natural Language Processing (EMNLP 2014)*, 2014.
- [6] S. Hochreiter and J. Schmidhuber, "Long short-term memory," *Neural Comput.*, vol. 9, no. 8, pp. 1735–1780, Nov. 1997. [Online]. Available: <http://dx.doi.org/10.1162/neco.1997.9.8.1735>

- [7] A. Jain, A. Singh, H. S. Koppula, S. Soh, and A. Saxena, "Recurrent neural networks for driver activity anticipation via sensory-fusion architecture," in *2016 IEEE International Conference on Robotics and Automation (ICRA)*, May 2016, pp. 3118–3125.
- [8] A. Jain, A. R. Zamir, S. Savarese, and A. Saxena, "Structural-rnn: Deep learning on spatio-temporal graphs," in *The IEEE Conference on Computer Vision and Pattern Recognition (CVPR)*, June 2016.
- [9] E. Galceran, A. G. Cunningham, R. M. Eustice, and E. Olson, "Multi-policy decision-making for autonomous driving via changepoint-based behavior prediction," in *Proceedings of Robotics: Science and Systems (RSS)*, Rome, Italy, July 2015.
- [10] J. Schlechtriemen, A. Wedel, J. Hillenbrand, G. Breuel, and K. D. Kuhnert, "A lane change detection approach using feature ranking with maximized predictive power," in *2014 IEEE Intelligent Vehicles Symposium Proceedings*, June 2014, pp. 108–114.
- [11] "ibeo lux fusion system," <https://autonomoustuff.com/product/ibeo-lux-fusion-system/>, accessed: 29th Aug, 2017.
- [12] J. P. Snyder, "Map projections: A working manual," US Government Printing Office, Tech. Rep., 1987.
- [13] C. M. Bishop, *Pattern Recognition and Machine Learning (Information Science and Statistics)*. Secaucus, NJ, USA: Springer-Verlag New York, Inc., 2006.
- [14] K. P. Murphy, *Machine Learning: A Probabilistic Perspective*. The MIT Press, 2012.
- [15] S. Nowozin, C. H. Lampert, *et al.*, "Structured learning and prediction in computer vision," *Foundations and Trends® in Computer Graphics and Vision*, vol. 6, no. 3–4, pp. 185–365, 2011.
- [16] J. L. Ba, J. R. Kiros, and G. E. Hinton, "Layer normalization," *arXiv preprint arXiv:1607.06450*, 2016.
- [17] S. Semeniuta, A. Severyn, and E. Barth, "Recurrent dropout without memory loss," *arXiv preprint arXiv:1603.05118*, 2016.
- [18] D. Kingma and J. Ba, "Adam: A method for stochastic optimization," *arXiv preprint arXiv:1412.6980*, 2014.
- [19] M. Abadi, A. Agarwal, P. Barham, and *et al.*, "TensorFlow: Large-scale machine learning on heterogeneous systems," 2015, software available from tensorflow.org. [Online]. Available: <https://www.tensorflow.org/>
- [20] M. M. Minderhoud and P. H. Bovy, "Extended time-to-collision measures for road traffic safety assessment," *Accident Analysis & Prevention*, vol. 33, no. 1, pp. 89–97, 2001.